

SUPPLEMENTARY INFORMATION

Ternary CBe₄Au₄ Cluster: A 16-Electron System with Quasi-Planar Tetracoordinate Carbon†

Jin-Chang Guo,^{‡ab} Lin-Yan Feng^{‡b} and Hua-Jin Zhai^{*b}

^a*Department of Chemistry, Xinzhou Teachers University, Xinzhou 034000, Shanxi, China*

^b*Nanocluster Laboratory, Institute of Molecular Science, Shanxi University, Taiyuan 030006, China*

E-mail: hj.zhai@sxu.edu.cn

‡ These authors contributed equally to this work.

Table S1. Orbital composition analysis of canonical molecular orbitals (CMOs) of the global-minimum structure **1** (C_{4v} , 1A_1) of CBe₄Au₄ cluster.

Table S2. Orbital composition analysis of delocalized π CMOs of the C_{4v} CBe₄M₄ (M = K, Au, H, Cl) series of quasi-planar tetracoordinate carbon (quasi-ptC) clusters.

Table S3. Orbital composition analysis of HOMOs of the T_d CBe₄M₄ (M = K, Au, H, Cl) series of tetrahedral carbon (thC) clusters.

Figure S1. Optimized ptC or quasi-ptC global-minimum structures **1–3** of CBe₄Au₄^{0/-2-} clusters and their three lowest-lying isomers (**nB–nD**) at the B3LYP/def2-TZVP level. Relative energies are listed in kcal mol⁻¹ at the single-point CCSD(T) level, with zero-point energy (ZPE) corrections at B3LYP.

- Figure S2.** Wiberg bond indices (WBIs) for **1–3** of $\text{CBe}_4\text{Au}_4^{0/-/2-}$ clusters from natural bond orbital (NBO) analyses.
- Figure S3.** Selected optimized salt complexes, $\text{CBe}_4\text{Au}_4\text{Na}^-$ and $\text{CBe}_4\text{Au}_4\text{Na}_2$ at B3LYP/def2-TZVP level, which are based on dianion $\text{CBe}_4\text{Au}_4^{2-}$ (**3**) cluster.
- Figure S4.** WBIs for selected structures of $\text{CAI}_4^{0/-/2-}$ clusters (**4–8**).
- Figure S5.** Optimized quasi-ptC C_{4v} structures **9–11** of CBe_4M_4 ($\text{M} = \text{K}, \text{H}, \text{Cl}$) and their T_d counterparts at the B3LYP/def2-TZVP level, as compared to those of CBe_4Au_4 and CAI_4 . Bond distances are given in angstroms. Natural atomic charges (in $|e|$) are shown in *italic* in red color. Relative energies are listed in kcal mol^{-1} at the single-point CCSD(T) level, with zero-point energy (ZPE) corrections at B3LYP.
- Figure S6.** WBIs for selected structures of CBe_4M_4 ($\text{M} = \text{K}, \text{Au}, \text{H}, \text{Cl}$) and CAI_4 .
- Figure S7.** Nucleus independent chemical shifts (NICSs) for clusters **1–3**. NICS(0) is calculated at the center of a triangle. NICS(1), shown in red color, is calculated at 1 Å above the center of a triangle or above the C center.
- Figure S8.** Canonical molecular orbitals (CMOs) of two typical structures of the 16-electron CAI_4 cluster. (a) C_{2v} (**5**). (b) T_d (**4**).

Table S1. Orbital composition analysis of canonical molecular orbitals (CMOs) of the global-minimum structure **1** (C_{4v} , 1A_1) of CBe_4Au_4 cluster. Main components are shown in bold.

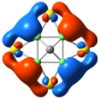

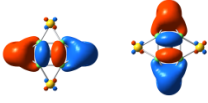

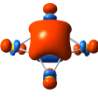
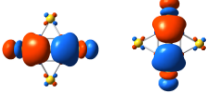
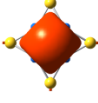

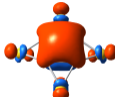


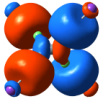
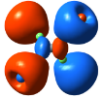
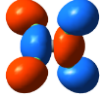
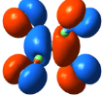
Subsystem	CMO	C (%)		Be ₄ (%)		Au ₄ (%)	
		s/p	total	s/p	total	s/d	total
LUMO	 LUMO (b_1)	0.0/0.0	0.0	23.5/57.3	80.8	0.0/19.2	19.2
Be-Au-Be 3c-2e σ	 HOMO-2 (b_2)	0.0/0.0	0.0	0.0/29.4	29.4	48.0/22.6	70.6
	 HOMO-1 (e)	0.0/33.2	33.2	2.7/18.5	21.2	40.5/5.1	45.6
	 HOMO-3 (a_1)	1.8/0.5	2.3	15.4/4.5	19.9	32.2/45.6	77.8
2 π aromaticity	 HOMO (a_1)	5.2/55.2	60.4	2.3/23.5	25.8	3.0/10.8	13.8
6 σ aromaticity	 HOMO-19 (e)	0.0/31.7	31.7	7.2/15.9	23.1	9.1/36.1	45.2
	 HOMO-20 (a_1)	59.6/3.1	62.7	14.9/19.3	34.2	1.3/1.8	3.1

Table S2. Orbital composition analysis of delocalized π CMOs of the C_{4v} CBe_4M_4 ($M = K, Au, H, Cl$) series of quasi-planar tetracoordinate carbon (quasi-ptC) clusters. Main components are shown in bold.

CBe_4M_4	CMO	C (%)		Be_4 (%)		M_4 (%)	
		s/p	total	s/p	total	s/p,d	total
CBe_4K_4	 HOMO-3 (a_1)	2.5/ 62.5	65.0	4.8/ 29.1	33.9	1.0/0.1	1.1
CBe_4Au_4	 HOMO (a_1) ^a	5.2/ 55.2	60.4	2.3/ 23.5	25.8	2.9/ 10.9	13.8
CBe_4H_4	 HOMO (a_1)	4.1/ 48.2	52.3	8.8/ 31.9	40.7	7.0/0.0	7.0
CBe_4Cl_4	 HOMO (a_1)	3.6/ 59.4	63.0	1.7/ 20.8	22.5	0.0/ 14.5	14.5

^a HOMO of CBe_4Au_4 is the most delocalized among all species listed, with major components from C, Be_4 , and Au_4 . Such delocalization, even with formally antibonding contribution from Au_4 (due to energy mismatch between atomic orbitals of Be and Au), helps stabilize the 2π system. It is the extent of spatial delocalization that matters.

Table S3. Orbital composition analysis of HOMOs of the T_d CBe_4M_4 ($M = K, Au, H, Cl$) series of tetrahedral carbon (thC) clusters. Main components are shown in bold.

CBe_4M_4	CMO ^a	C (%)		Be ₄ (%)		M ₄ (%)	
		s/p	total	s/p	total	s/p,d	total
CBe_4K_4	 HOMO (t_2)	0.0/3.8	3.8	31.9/30.9	62.8	32.8/0.6	33.4
CBe_4Au_4	 HOMO (t_2)	0.00/4.1	4.1	7.5/ 12.7	20.2	59.1/16.6	75.7
CBe_4H_4	 HOMO (t_2) ^b	0.0/ 35.6	35.6	3.1/ 17.4	20.5	43.9/0.0	43.9
CBe_4Cl_4	 HOMO (t_2)	0.0/ 33.6	33.6	2.3/1.7	4.0	0.0/ 62.4	62.4

^a HOMO orbitals of T_d CBe_4M_4 ($M = K, Au, H, Cl$) clusters are triply degenerate, and only one component is depicted and compared in the table.

^b Compared to those of other species, HOMO of T_d CBe_4H_4 has prominent C-Be-H σ conjugation with major orbital components from C, Be₄, and H₄. This effect stabilizes T_d CBe_4H_4 as the global minimum, in contrast to CBe_4Au_4 that has C_{4v} geometry (see Fig. 7 and also footnote in Table S2).

Figure S1. Optimized ptC or quasi-ptC global-minimum structures **1–3** of $\text{CBe}_4\text{Au}_4^{0/-2-}$ clusters and their three lowest-lying isomers (**nB–nD**) at the B3LYP/def2-TZVP level. Relative energies are listed in kcal mol^{-1} at the single-point CCSD(T) level, with zero-point energy (ZPE) corrections at B3LYP.

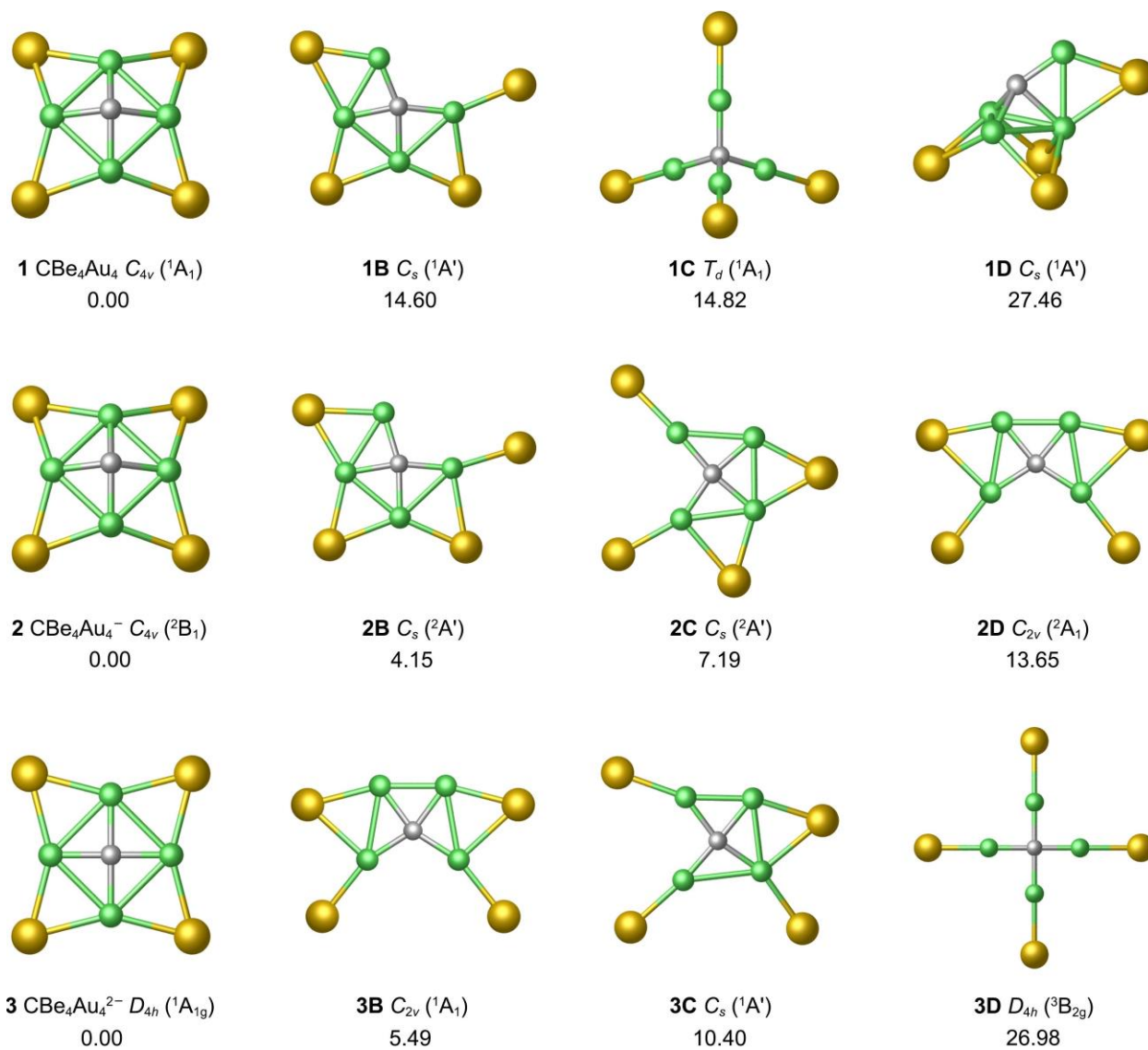
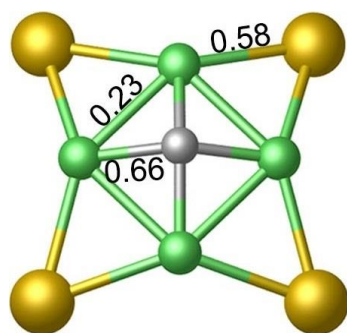
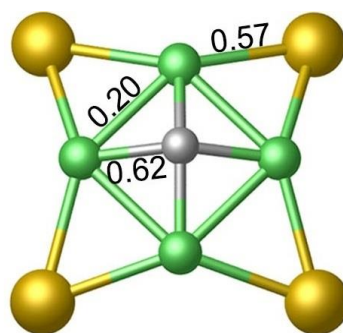


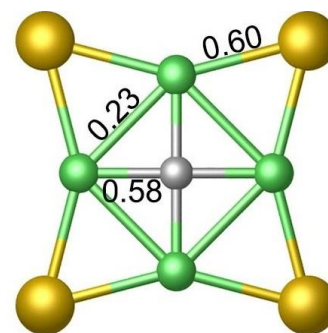
Figure S2. Wiberg bond indices (WBIs) for **1–3** of $\text{CBe}_4\text{Au}_4^{0/-/2-}$ clusters from natural bond orbital (NBO) analyses.



1 C_{4v} CBe_4Au_4



2 C_{4v} $\text{CBe}_4\text{Au}_4^-$



3 D_{4h} $\text{CBe}_4\text{Au}_4^{2-}$

Figure S3. Selected optimized salt complexes, $\text{CBe}_4\text{Au}_4\text{Na}^-$ and $\text{CBe}_4\text{Au}_4\text{Na}_2$ at B3LYP/def2-TZVP level, which are based on dianion $\text{CBe}_4\text{Au}_4^{2-}$ (**3**) cluster.

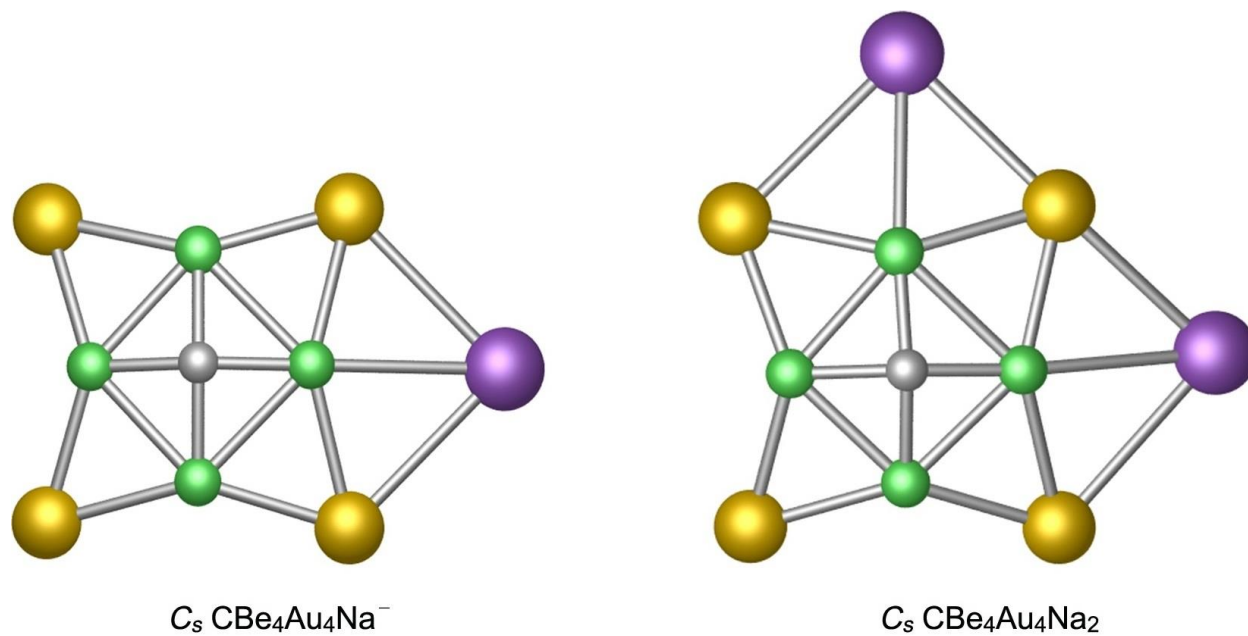


Figure S4. WBIs for selected structures of $\text{CaI}_4^{0/-/2-}$ clusters (**4–8**).

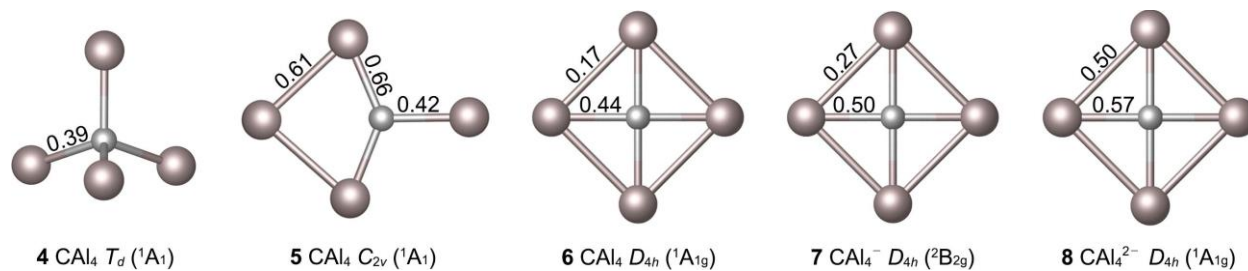


Figure S5. Optimized quasi-ptC C_{4v} structures **9–11** of CBe_4M_4 ($M = K, H, Cl$) and their T_d counterparts at the B3LYP/def2-TZVP level, as compared to those of CBe_4Au_4 and CAI_4 . Bond distances are given in angstroms. Natural atomic charges (in $|e|$) are shown in *italic* in red color. Relative energies are listed in kcal mol⁻¹ at the single-point CCSD(T) level, with zero-point energy (ZPE) corrections at B3LYP.

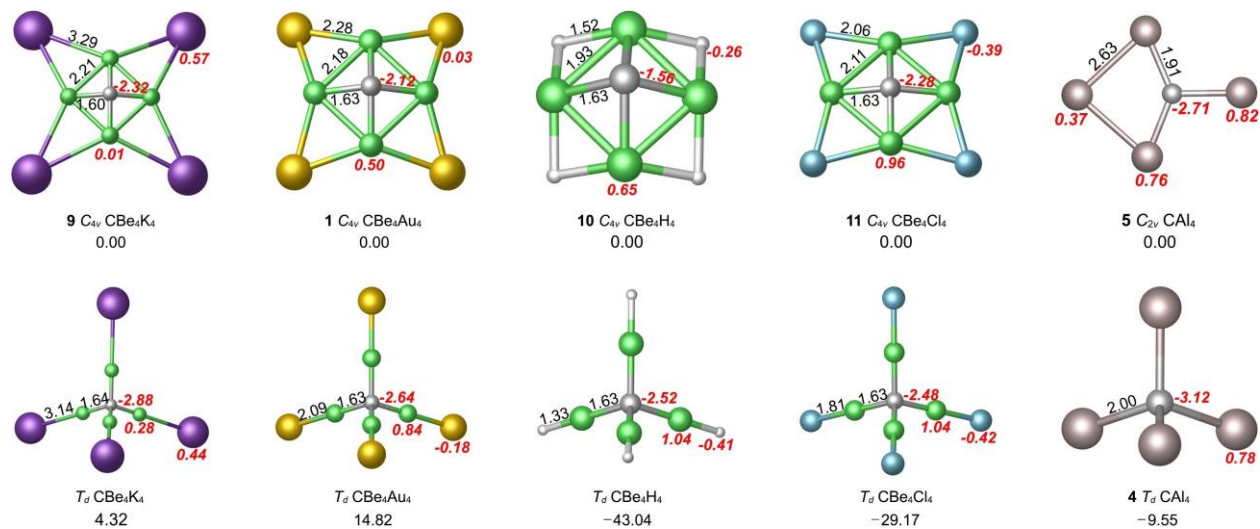


Figure S6. WBIs for selected structures of CBe_4M_4 ($\text{M} = \text{K}, \text{Au}, \text{H}, \text{Cl}$) and CAI_4 .

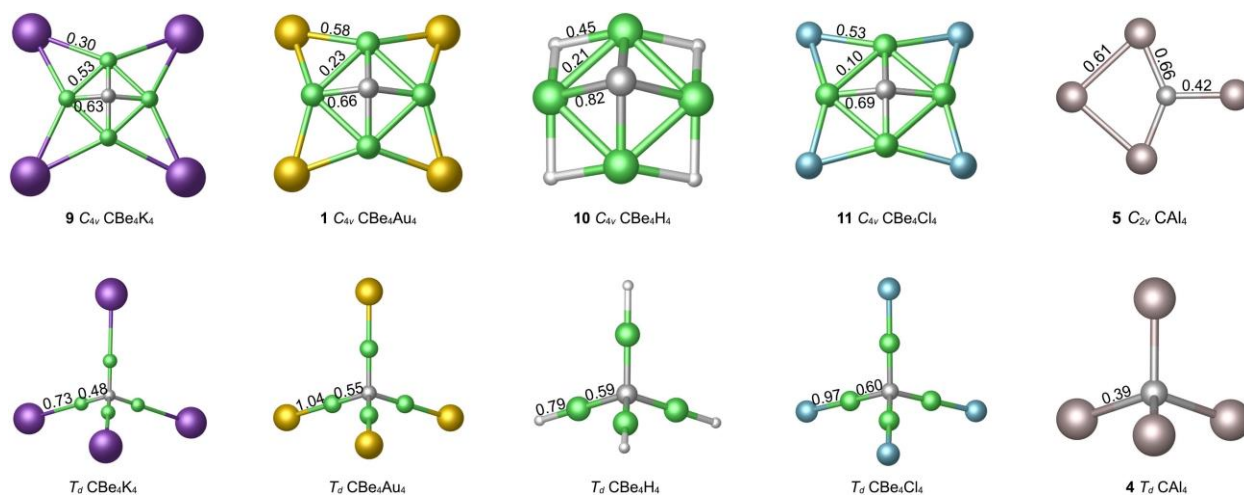


Figure S7. Nucleus independent chemical shifts (NICSs) for clusters **1–3**. NICS(0) is calculated at the center of a triangle. NICS(1), shown in red color, is calculated at 1 Å above the center of a triangle or above the C center.

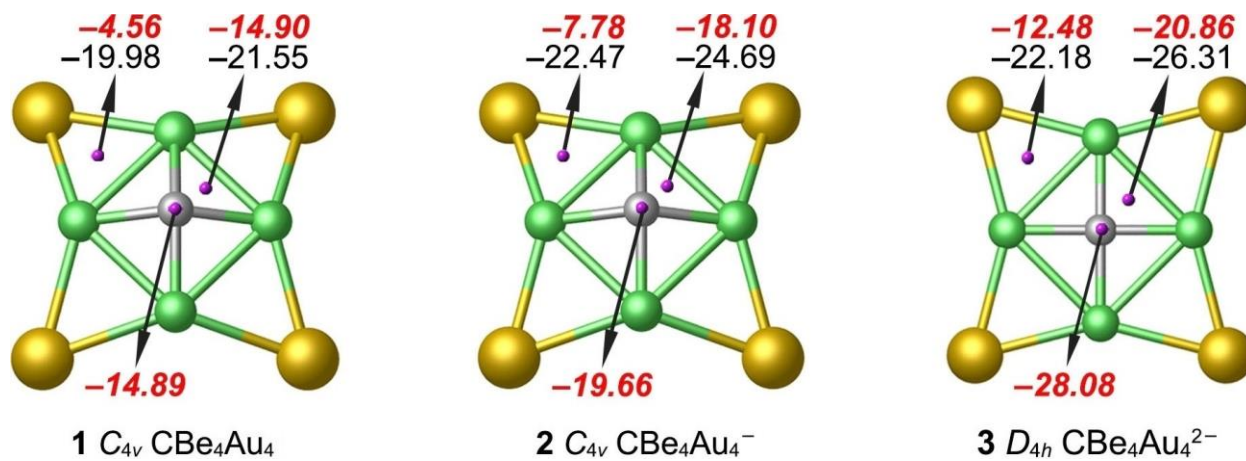


Figure S8. Canonical molecular orbitals (CMOs) of two typical structures of the 16-electron CaI_4 cluster. (a) C_{2v} (**5**). (b) T_d (**4**).

